Characterization of the Low-Field Proton Magnetic Resonance Spectrum of Plasminogen Kringle 4 via Selective Overhauser Experiments in ^1H_2O†

Andrea Motta,‡,§ Richard A. Laursen,‖ and Miguel Llinás*,‡

Department of Chemistry, Carnegie-Mellon University, Pittsburgh, Pennsylvania 15213, and Department of Chemistry, Boston University, Boston, Massachusetts 02215

Received June 11, 1986; Revised Manuscript Received August 14, 1986

ABSTRACT: The low-field ^1H NMR spectrum of the kringle 4 domain of human plasminogen has been investigated at 300 and 600 MHz for the protein dissolved in ^1H_2O. The spectrum exhibits six well-resolved resonances, spanning the $9.8 \lesssim \delta \lesssim 13$ ppm chemical shift range, which arise from exchange-labile H atoms. The acid–base response of the six resonances was monitored in order to characterize the signals in terms of their pH titration profiles. The sensitivity of the low-field resonances to kringle binding the antifibrinolytic ligands N^{α}-acetyl-L-lysine and *p*-benzylaminesulfonic acid was also investigated. The lowest field resonance, at 12.6 ppm, is a doublet of $J \sim 7.9$ Hz, a splitting that is unprecedented for His or Trp ring NH signals. Selective Overhauser experiments centered on the exchangeable proton transitions identify four of the other resonances as stemming from the His^{31}, His^{33}, Trp I, and Trp II side-chain NH groups, where the latter two are, as yet, not definitely assigned to the specific residues, Trp^{25} and Trp^{62}. The relative narrowness of the His imidazole NH signals indicates that the two rings are sterically shielded from direct water accessibility. In particular, the His^{33} NH site appears to be the most protected. The Overhauser evidence conclusively shows that the two identified exchangeable His ring proton signals arise from imidazole NH3 sites rather than from the NH1 tautomers. Similarly, these experiments lead to an unambigous characterization of the corresponding Trp aromatic CH spin systems. In the absence of ligand, the Trp I (Trp^{25}?) NH1 resonance is shifted ~0.9 ppm from the corresponding Trp II (Trp^{62}?) signal, the latter being positioned closer to the characteristic "random-coil" Trp indole NH1 chemical shift. Trp I is hence significantly more buried within the structure, which is consistent with its retarded rate of isotope exchange in ^2H_2O solution and with the overall spread of its aromatic CH spectrum. The remaining low-field resonance that was investigated remains unidentified. The latter signal and that from the Trp II indole NH1 are shown to be the most sensitive to ligand binding. These observations, in combination with other characteristics (line width, H-exchange lability, etc.), suggest that the two resonances arise from groups relatively exposed at the ligand-binding site.

The fourth kringle domain of human plasminogen carries a lysine-binding site (Sottrup-Jensen et al., 1978), which also binds a number of antifibrinolytic drugs and other ω-amino acid analogues of lysine, such as ε-aminocaproic acid, N^{α}-acetyl-L-lysine (AcLys),[1] BASA, etc. (Lerch et al., 1980; Winn et al., 1980; Hochschwender et al., 1983). The structure of the kringles' lysine-binding site is a matter of considerable interest, from both biochemical and clinical standpoints, since it is thought that kringle domains are directly involved in establishing the interaction between plasmin(ogen) and its target substrate, polymerized fibrin within blood clots (Wiman & Wallén, 1977; Thorsen et al., 1981).

In the absence of a detailed crystallographic picture of the kringle 4 structure, much of our understanding of the molecular factors determining the lysine-binding site specificity has resulted from kringle sequence homology arguments, chemical modification experiments, and ^1H NMR spectroscopic studies. The preliminary model that has evolved points to two main classes of contributors to the binding site structure: (a) polar amino acids such as His^{31} and Asp^{55} (Lerch & Rickli, 1980) or Arg^{71} and Asp^{57} (Trexler et al., 1982), providing basic and acidic side-chain groups that can pair electrostatically to the ligand dipole charges; (b) hydrophobic residues, such as Trp^{72} (Hochschwender & Laursen, 1981), Trp II (Trp^{62} or Trp^{25}), and Phe^{64} and Tyr^{74} (Llinás et al., 1985; De Marco et al., 1986a; V. Ramesh, R. A. Laursen, and M. Llinás, unpublished observations), which afford aromatic contact surfaces to interact with the hydrocarbon moieties of the ligands. A central feature of the model is the loop stretching from Cys^{51} to Cys^{75}, which encompasses the lysine-binding site. Furthermore, the NMR evidence indicates that other residues, including Leu^{46}, Trp I (Trp^{25} or Trp^{62}), His II (His^{31}), His III (His^{33}), and Tyr III (Tyr^{41}), are either at, or are contiguous to, the lysine-binding site (Llinás et al., 1985; De Marco et al., 1986a). These residues are known to be in close proximity with one another and thus define a hydrophobic core that furnishes structural stability to the kringle fold (De Marco et al., 1985a,b).

All previous NMR studies of plasminogen kringles have dealt with ^2H_2O solutions of the isolated domains. In so doing, resonances arising from exchange-labile NH groups were purposely eliminated from the spectrum in order to simplify

† This research was supported by the U.S. Public Health Service, NIH Grants HL 15535 and HL 29409. The 600-MHz NMR facility is supported by Grant RR 00292 from the National Institutes of Health.

‡ Carnegie-Mellon University.

§ Permanent address: Istituto per la Chimica di Molecole di Interesse Biologico, Consiglio Nazionale delle Ricerche, Napoli, Italy.

‖ Boston University.

[1] Abbreviations: AcLys, N^{α}-acetyl-L-lysine; BASA, *p*-benzylaminesulfonic acid; CIDNP, chemically induced dynamic nuclear polarization; FID, free induction decay; K4, kringle 4; NOE, nuclear Overhauser effect; pH*, glass electrode pH reading uncorrected for deuterium isotope effect; ppm, parts per million; rf, radio frequency; 2D, two-dimensional; TSP, sodium 3-(trimethylsilyl)[2,2,3,3-$^2H_4$]propionate.

0006-2960/86/0425-7924$01.50/0

the low-field ($\delta \gtrsim 5$ ppm) spectral region, which contains most of the aromatic resonances. However, the cost of such a procedure is a loss of NH signals stemming from His imidazole, Trp indole, and peptidyl amide groups. Because of their high sensitivity to electrostatic and H-bonding interactions, these resonances have the potential of providing valuable structural information when kringle–ligand interactions are investigated. These exchangeable resonances can, however, be seen by studying the protein in ^1H_2O solutions. Furthermore, ^1H NMR studies in ^1H_2O afford the possibility to characterize the kringle Trp indole spectra. To date, the indole proton spectrum of only Trp I (Trp^{25} or Trp^{62}) has been unambiguously assigned (De Marco et al., 1985c). In the cases of Trp II (Trp^{62} or Trp^{25}) and Trp III (Trp^{72}), the individual aromatic subspectra have been identified in terms of doublet–triplet–triplet–doublet connectivities, but absolute assignments of specific multiplets, e.g., CH4 or CH7 (doublets) and CH5 or CH6 (triplets), is lacking.

This paper provides a first description of the low-field ^1H NMR spectrum of kringle 4 in ^1H_2O. Six resonances, all arising from exchange-labile hydrogens, are found to be conveniently resolved within the $9.8 \lesssim \delta \lesssim 13$ ppm range. Proton Overhauser experiments based on the selective irradiation of these transitions lead to the identification of three of these signals as arising from Trp II, His II (His^{31}), and His III (His^{33}) side-chain groups. Two of the remaining resonances are likely to be due to an amide NH proton and a yet unidentified group. The sixth NH signal arises from the Trp I indole ring, in agreement with an earlier Overhauser experiment in ^2H_2O (De Marco et al., 1985c). The effect of ligand binding as well as of acid–base perturbation on these signals was also investigated. The data are discussed in terms of resonance assignments and of their implications for the structure of the lysine-binding site. In an accompanying paper (De Marco et al., 1986b), we discuss 2D photo-CIDNP experiments in ^2H_2O, which totally assign the Trp III (Trp^{72}) indole CH spectrum.

Materials and Methods

Kringle 4 was generated by elastase fragmentation of human plasminogen (Sottrup-Jensen et al., 1978) as published (Winn et al., 1980). AcLys was purchased from Sigma, and BASA was prepared as described by Hochschwender et al. (1983).

Fourier ^1H NMR spectra were recorded at 300 MHz with a Bruker WM-300 spectrometer and at 600 MHz with the National NMR Facility for Biomedical Studies at Carnegie-Mellon University. Protein solutions were 10^{-3} M in ^1H_2O or ^2H_2O. Dioxane was used as internal reference and assumed to resonate at 3.766 ppm relative to TSP (De Marco, 1977). All spectra were acquired with quadrature detection, and resolution enhancement, whenever implemented, was achieved via Gaussian convolution (Ernst, 1966; Ferrige & Lindon, 1978). The dynamic range problem caused by the presence of the strong ^1H_2O peak was overcome by applying rf excitation with zero-power spectral density at the water resonance position. At 600 MHz, the spectra were acquired by use of a long, weak ("soft") pulse of length L (Alexander, 1968; Redfield & Gupta, 1971), whose Fourier-transform is proportional to $\sin[(\omega_{H_2O} - \omega_{carrier})L]/(\omega_{H_2O} - \omega_{carrier})L$. L was chosen such as to include the spectral region containing the exchangeable and the aromatic resonance protons within the two first rf power nodes, i.e., within $\pm 0.97/L$ Hz from the carrier (Alexander, 1968). The 300-MHz spectra were acquired with the 1–1 pulse sequence (Clore et al., 1983). The latter involves two "hard" $\pi/4$ pulses of equal phase separated by a time gap of length τ. The spectrum of such excitation

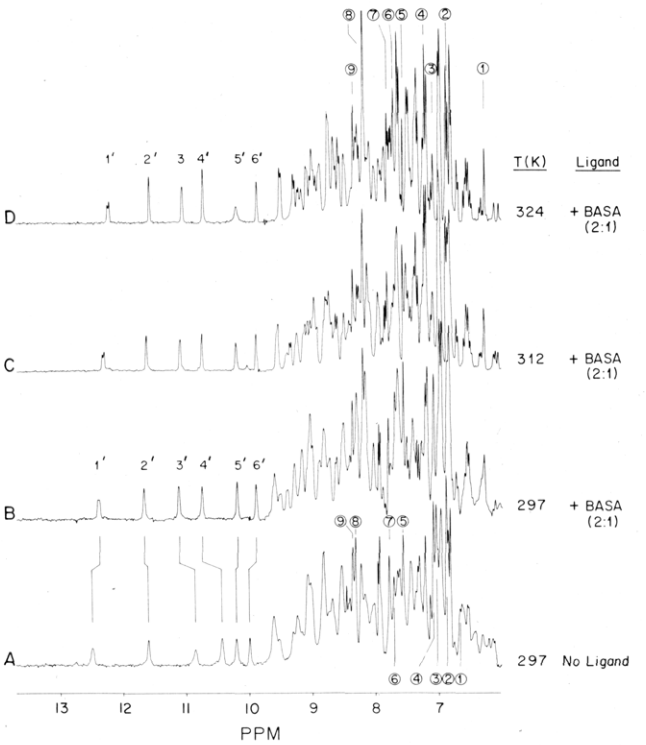

FIGURE 1: ^1H NMR low-field spectra of kringle 4 in ^1H_2O, at 300 MHz: ligand and temperature effects. (A) Ligand-free kringle 4 at 297 K. The nine aromatic CH singlets are labeled with circled numbers (De Marco et al., 1985c). (B–D) Kringle 4 in presence of 2:1 excess BASA at 297 (B), 312 (C), and 324 K (D). Low-field exchangeable resonances are numbered 1′–6′. BASA-induced resonance shifts are indicated by broken vertical lines connecting spectra A and B. Kringle concentration $\sim 10^{-3}$ M, pH 7.1. Each spectrum represents an average of 2000 scans and is shown resolution-enhanced.

is amplitude-modulated according to $\cos[(\omega_{H_2O} - \omega_{carrier})\tau/2]$, which introduces rf power nodes at $(\omega_{H_2O} - \omega_{carrier}) = n\pi/\tau$, where $n = \pm 1, \pm 3, \ldots$. Because of the periodicity of the spectral density function, the carrier can be positioned symmetrically at either side of the ^1H_2O signal. This feature is advantageous for Overhauser experiments, as it makes it possible to set the "observe" carrier frequency, relative to the selectively irradiated transition, at the other side of the water signal. It was empirically noticed that, in this way, additive effects between the preirradiation and observe pulses, which can affect the position of the ^1H_2O null in an erratic fashion, are avoided. Base-line distortions were minimized by deleting the first few points of the FID, which usually appear as spikes (Roth et al., 1980).

All the Overhauser experiments are shown as difference (unperturbed minus perturbed) spectra. Truncated driven Overhauser experiments (Dubs et al., 1979) were run by preirradiating a transition for a fixed time, typically 0.5 s, before sampling with the 1–1 pulse. The frequency setting of the preirradiation pulse was alternated between off- and on-resonance spectral positions every eight scans, and the resulting FIDs were subtracted in computer memory to minimize long-term instrumental instability artifacts. Several thousand eight-scan cycles were acquired in order to achieve a satisfactory signal-to-noise ratio.

Results and Discussion

Figure 1A shows the low-field ^1H-NMR spectral region of kringle 4 in ^1H_2O, pH 7.1, recorded at 300 MHz, 297 K. Within this region, the area between 9.5 and 6.0 ppm includes most of the aromatic CH spectrum and resonances from backbone peptidyl amide NH groups and from other poten-

tially protected exchange-labile groups such as side-chain OH and NH groups. Despite the major signal overlap, the sharp CH aromatic singlets, originating from the His imidazole CH2 and CH4 and from the Trp indole CH2, can be readily identified from their positions in the corresponding spectrum in ^2H_2O (De Marco et al., 1985c) and are numbered 1–9 (labels enclosed in circles) in Figure 1A,D. Between 13 and 10 ppm, six well-resolved, isolated signals are observed; these have been numbered 1′–6′ in Figure 1B,D.

The $\delta \lesssim 10$ ppm region usually contains signals stemming from Trp indole and His imidazole groups as well as shifted resonances from backbone peptidyl NH groups. Spectra B–D in Figure 1 differ from spectrum A in that a 2-fold molar excess of the ligand BASA has been added to the kringle sample. As previously observed for kringle 4 in ^2H_2O (Hochschwender et al., 1983), the addition of ligand brings about a generalized sharpening of peaks in the spectrum; this is readily detected on the exchangeable peaks 1′–6′, being most noticeable for peak 3′ (Figure 1B). When the temperature is raised from 297 to 324 K, further narrowing occurs and helps to resolve peak 1′, which now appears as a neat doublet ($J \sim 7.9$ Hz) shifted to high-field ~–0.11 ppm (Figure 1B–D). Its low-field position could reflect H bonding of the NH group as well as local conformational features, such as anisotropic deshielding effects from neighboring aromatic rings. However, peak 1 exhibits fast exchange in ^2H_2O (Hochschwender et al., 1983), suggesting that the site is relatively exposed to solvent. Since the decrease of the spectral line widths with increasing temperature is so generalized, the broadening at 324 K of resonances 5′ and, to a lesser degree, 3′ appears to be anomalous. This behavior most likely reflects a thermally activated dynamic process such as H exchange with the solvent (^1H_2O) *or* a modulation of its chemical shift caused by internal motions.

The vertical lines connecting spectra A and B (Figure 1) indicate ligand-induced shifts on the resonances 1′–6′. In order to determine the relationship of these residues to the ligand-binding site, Overhauser experiments were implemented with the aim of identifying the origin of the resonances in ^1H_2O. Difference spectra resulting from irradiating transitions 1′–6′ (at pH 7.1, 297 K) are shown in Figure 2. Irradiation of peak 2′ at 11.60 ppm (spectrum B) perturbs signals at 7.14 and at 7.45 ppm. On the basis of an analogous experiment in ^2H_2O, this pair of resonances has been assigned to the Trp I ring CH2 (singlet 4) and CH7 (doublet) (De Marco et al., 1985c), a result that is to be expected when a Trp indole NH1 is irradiated (Poulsen et al., 1980). Thus, the experiment demonstrates that resonance 2′ arises from the Trp I NH1 proton. A similar pattern results on irradiation of peak 4′ (Figure 2D), yielding NOEs at ~7.80 (singlet 7) and at ~7.05 ppm (doublet).

Pr^{3+}-induced shifts observed by N. D. Pluck and R. J. P. Williams (unpublished results) and Overhauser experiments in ^2H_2O (De Marco et al., 1985c) have suggested that the CH singlet 7 (Figure 1A), which is noticed in the NOE spectrum at ~7.80 ppm (Figure 2D), should be paired to the Trp II aromatic spectrum. However, the problem of identifying the CH7 doublet within the latter indole spin system remains unsolved. Once one of the Trp II indole multiplets is identified, the rest of the aromatic spectrum becomes assigned as the intraresidue scalar spin–spin connectivities have been established via 2D spectroscopy (De Marco et al., 1985c; Ramesh et al., 1986). Figure 3 displays Overhauser difference spectra resulting from irradiation of NH peak 4′ in the absence (A) and in the presence (B) of BASA. Both experiments show

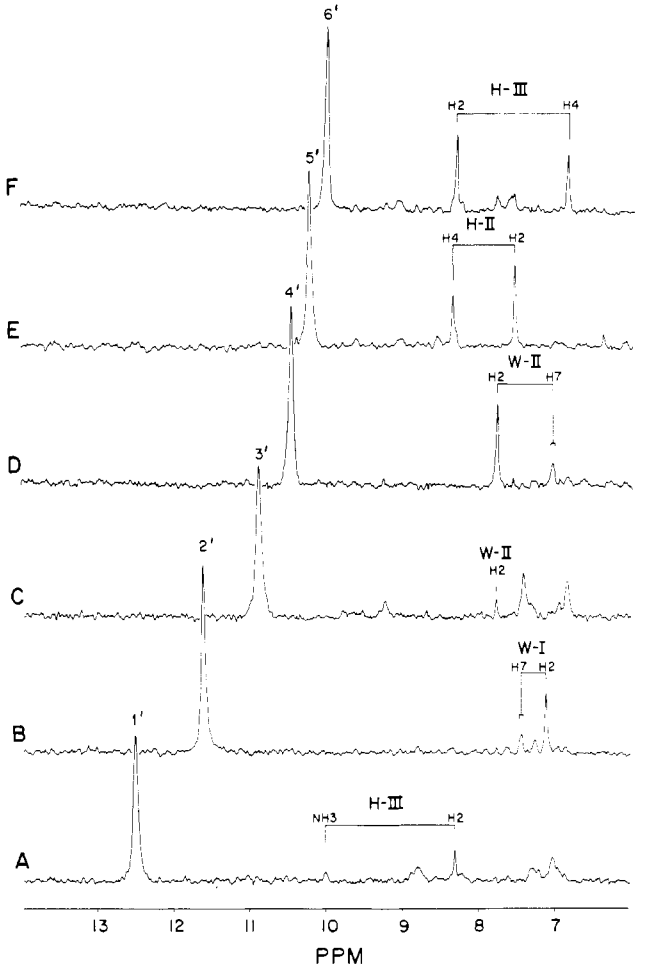

FIGURE 2: Kringle 4 proton Overhauser experiments in ^1H_2O at 300 MHz. (A–F) NOE difference spectra resulting from irradiation of NH resonances 1′–6′ (see Figure 1A). The correspondence between identified NOE signals and proton positions in the aromatic rings are indicated following the conventional one-letter code as used in previous papers (Llinás et al., 1983; De Marco et al., 1985c). A preirradiation pulse was applied for 0.5 s on- and off-resonance before sampling; 2-s recycling time. Each spectrum represents an average of 8000 scans off-resonance minus 8000 scans on-resonance, so that negative NOEs show with positive sign. Kringle concentration ~1.5×10^{-3} M, pH 7.1, 297 K.

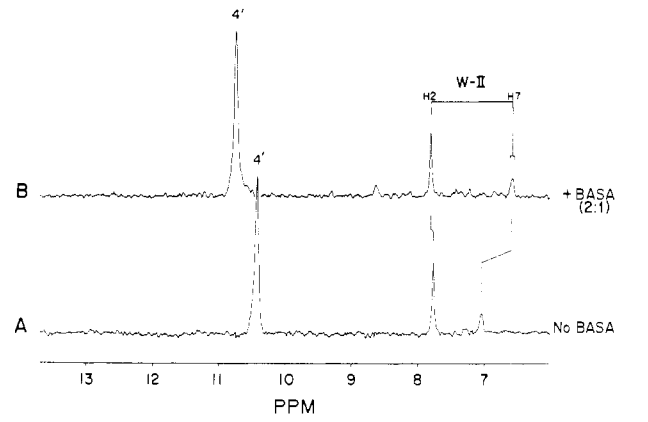

FIGURE 3: Kringle 4 NOE difference spectra in ^1H_2O at 300 MHz: Trp II identification. (A) Ligand-free kringle 4; (B) kringle 4 in the presence of a 2-fold molar excess of BASA. The irradiated indole NH1 peak is labeled 4′; the identified Trp II CH2 singlet and CH7 doublet are labeled W-II in spectrum B. Broken lines connecting spectra A and B indicate resonance shifts induced by BASA. Experimental conditions are those described for Figure 2.

a response from a singlet (indole CH2) and a doublet (indole CH7) whose correspondences in Figure 3 are indicated. In

Scheme I: Histidyl Imidazole Tautomers and Acid/Base Equilibrium Forms

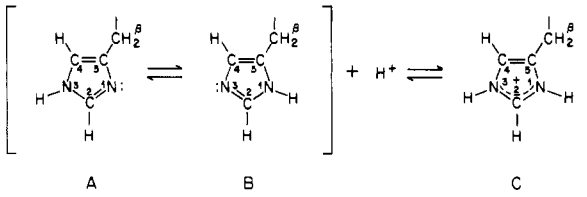

A B C

the absence of BASA, indole doublets of Trp II and of Trp III appear very close at 7.05 and at 7.0. ppm, respectively (De Marco et al., 1985c). Since BASA shifts the Trp II doublet upfield and the Trp III doublet downfield (Llinás et al., 1985), the signal at 7.05 ppm (6.57 ppm in the presence of BASA) becomes assigned to the Trp II indole CH7 group and is paired to the CH2 singlet at 7.80 ppm.

Irradiation of a His imidazole NH3 transition is expected to elicit NOEs on the ring CH2 and CH4 singlets while irradiation of the corresponding NH1 should only affect the CH2 signal (see Scheme I). As shown by Figure 2E, irradiation of peak 5′ elicits response from the two singlets at 8.35 and 7.55 ppm, which correspond to the CH4 and CH2 signals of His II (His^{31}), respectively (singlets 9 and 5 in Figure 1A). The reversed ordering of the His II CH resonances has been discussed elsewhere (Llinás et al., 1983; De Marco et al., 1985c). Overhauser enhancements on two imidazole CH singlets are also observed when peak 6′ is irradiated (Figure 2F), and they correspond to the CH2 (8.31 ppm) and the CH4 (6.88 ppm) of His III (His^{33}) (singlets 8 and 2 in Figure 1A). Thus, the NOE difference spectra E and F in Figure 2 assign peaks 5′ and 6′ to NH3 protons from two of the three His imidazole groups found in kringle 4. These assignments were confirmed by repeating the experiments in the presence of BASA and correlating the NOE signals with the shifts induced by the ligand (De Marco et al., 1986a). In both cases, a slightly more efficient NOE is detected for the CH2 signal than for the CH4. Similar results have been observed in superoxide dismutase (Stoesz et al., 1979) and also in the case of kringle 1, when the NH3 of His^{31} is irradiated (our unpublished results).

The effects of irradiating peak 1′ (Figure 2A) are apparent at 8.32 and 9.99 ppm. The latter NOE is readily identified as arising from peak 6′, i.e., the imidazole NH3 of His III (His^{33}), while the one at 8.32 ppm could arise from either the His II (His^{31}) CH4 or the His III (His^{33}) CH2. However, a similar experiment in the presence of BASA leads to assignment of the peak to His III (His^{33}). Other effects are observed on resonances at ~7 ppm, which, from their broad appearance, would seem to originate from exchangeable, backbone amide NH groups. Thus, as discussed above, the doublet NH resonance 1′ (Figure 1B,C) is likely to stem from an exchangeable NH group proton that interacts closely with the His III (His^{33}) ring.

Irradiation of peak 3′ (Figure 2C) perturbs none of the His or Trp ring resonances so far discussed, except for the CH2 of Trp II. The peaks at 7.41 and 6.84 ppm have not been unambiguously assigned owing to crowding of signals in this area. On the basis of their chemical shifts and line widths, the two resonances could originate from the aromatic rings of Tyr III (Tyr^{41}) and Tyr II (Tyr^{50}) or Tyr IV (Tyr^{74}), which suggest that resonance 3′ could arise from a Tyr phenolic OH proton, buried within the structure. However, chemical modification studies have shown that Tyr^{41} and Tyr^{50} can be nitrated and therefore that their –OH groups must be relatively exposed (Trexler et al., 1985). Furthermore, photo-CIDNP experiments show polarization of the Tyr^{74} aromatic spectrum, so that this ring –OH group, too, should be somewhat accessible (De Marco et al., 1986b). Thus, although the evidence is inconclusive at this time, a peptidyl amide NH group would appear to be the most likely candidate for peak 3′.

So far we have unambiguously identified resonances originating from the Trp I and Trp II indole groups (peaks 2′ and 4′, respectively) and from the His II (His^{31}) and His III (His^{33}) imidazole rings (5′ and 6′, respectively). Kringle 4 contains one more each of a Trp (Trp^{72}) and His (His^{3}) residue, so that two such NH signals remain to be found. The pK_a of His^3 (His I) is 6.1 (De Marco et al., 1985c), which is that of a solvent-exposed His side chain (Markley, 1975). Such a pK_a, combined with the long relaxation time T_2 shown by its CH singlets (Llinás et al., 1983), indicates that the His^3 side chain is accessible to solvent and relatively mobile. Thus, we might not expect to observe the imidazole NH resonance of His^3 (His I) simply because of fast exchange broadening. In contrast, in small flexible peptides, the Trp indole NH is observed to yield a relatively sharp signal at 10.1 ppm within the range $2 \leq$ pH ≤ 8 (our unpublished observations). Chemical modification experiments on kringle 4 have shown that among the three Trp residues Trp^{72} is the only one that exhibits reactivity (Hochschwender & Laursen, 1981; Llinás et al., 1983; Trexler et al., 1983) so that its indole group must be relatively exposed to the solvent, as is the case with model peptides. Therefore, the Trp^{72} NH1 resonance is expected to be observable in ^1H_2O, pH 7.1, namely, the experimental conditions of our study. However, a systematic search for the corresponding indole NH signal by irradiating all the transitions between 9 and 10 ppm failed to elicit NOEs on singlet 1. On the other hand, this result probably is not too surprising since the aromatic spectrum of Trp^{72}, whether in the presence or absence of ligand, is definitely not that of a random-coil residue, most likely because of close contacts with other aromatic rings at the ligand-binding site. Thus, the Trp^{72} NH1 indole resonance may be shifted to a high-field position, where it would be obscured by the rest of the aromatic and amide NH spectrum.

Figure 4 shows pH effects on the kringle 4 low-field exchangeable NH spectrum at 600 MHz. The acid–base response was monitored within the range $10.8 \leq$ pH ≤ 3.2, whose upper and lower limits correspond to the pH values for half-unfolding so that within most of this range the protein is in its globular, native form (De Marco et al., 1985b). To avoid hysteresis effects, two identical samples, originating from the same protein batch, were titrated starting at pH 7.1: one was used for collecting data in the alkaline range while the other was monitored within the acidic range. On lowering the pH from 10.8 (Figure 4A) to 4.8 (Figure 4F), resonances 1′, 2′ (Trp I NH1), and 6′ (His III NH3) exhibit negligible changes in both line widths and chemical shifts. Only below pH 4.8 do they broaden (Figure 4G). However, at pH $\leq$4.8 kringle 4 begins to unfold (De Marco et al., 1985b), so that the broadening of these peaks is likely to arise from (fast) conformational exchange between folded and unfolded forms in equilibrium, which may also cause the small upfield shifts observed for resonances 1′ and 6′. Peak 3′, whose chemical shift is essentially acid–base insensitive, is very broad at pH 10.8, sharpens upon lowering the pH (Figure 4B–F), and broadens again slightly at pH <4.8, once more reflecting unfolding of the protein and possibly acid/base catalysis of H exchange (Figure 4G). Resonances 4′ (Trp II NH1) and 5′ (His II NH3) are the most sensitive to pH, showing both large shifts and broadening at low pH.

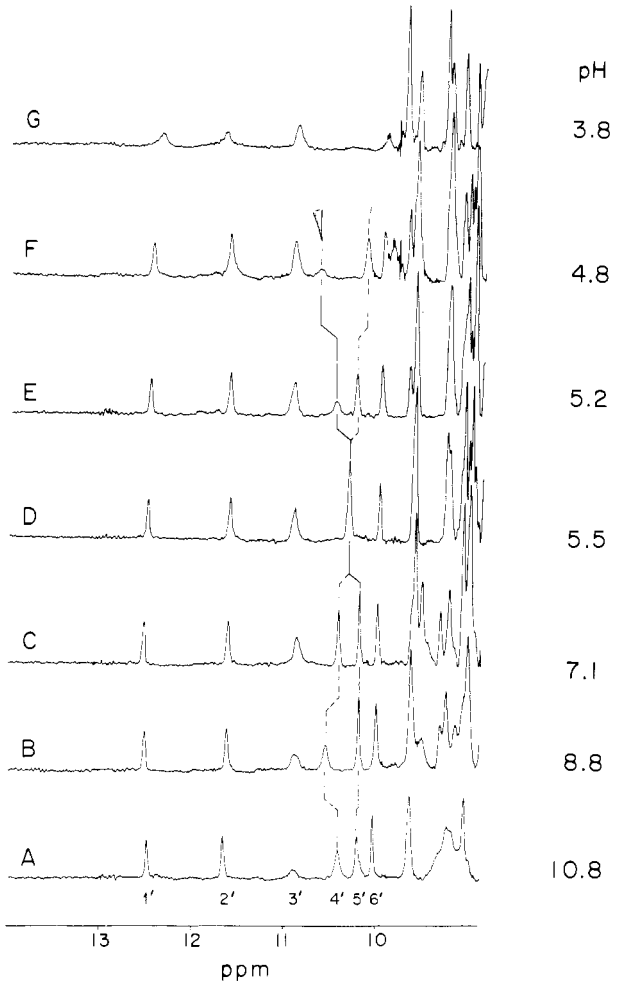

FIGURE 4: ^1H NMR low-field spectra of kringle 4 in ^1H_2O, at 600 MHz: acid–base perturbation of exchangeable protons. The six resonances under study are numbered 1′–6′ in spectrum A. Upon lowering of the pH, the largest shifts are observed for peaks 4′ (indicated by a dashed line) and 5′ (indicated by a continuous line). Resonances 4′ and 5′ broaden and eventually disappear on increasing the acidity below pH 7 (F and G). Kringle concentration $\sim 10^{-3}$ M, 297 K.

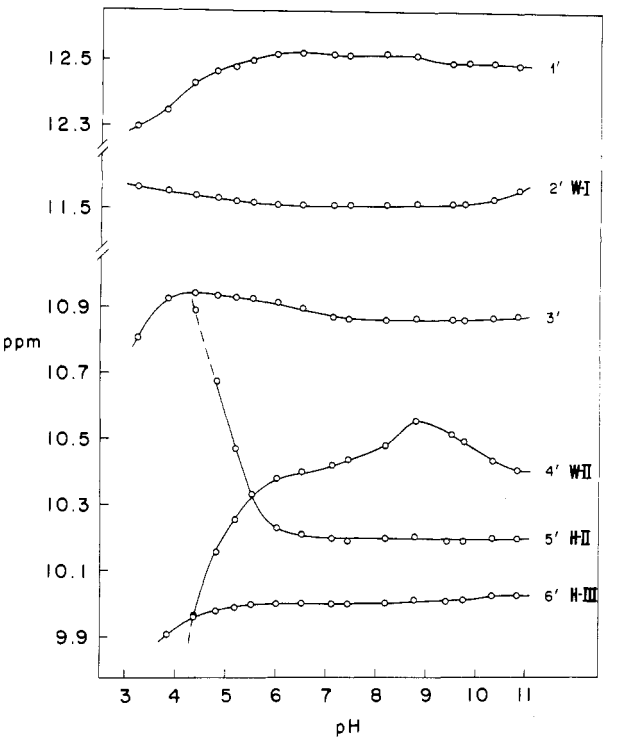

FIGURE 5: Chemical shift pH profile of the kringle 4 low-field proton resonances. The curves are numbered 1′–6′ in accord with the corresponding resonances in Figure 4, which shows a sample of experimental spectra. Kringle concentration $\sim 10^{-3}$ M, 295 K.

Figure 5 shows the chemical shift pH titration profiles for the six NH resonances under discussion. Peak 5′ (His^{31}) exhibits a most pronounced response below pH ~6, with an inflection that is consistent with a pK_a^* ~ 5.4 calculated from titration of the (His II) CH2 and CH4 singlets in ^2H_2O (De Marco et al., 1985c). The Trp II NH1 peak 4′ is also quite sensitive to pH: it exhibits a definite maximum within 8 < pH < 9.5 and a marked high-field shift for pH ≲6. Since the indole NH, per se, is not titratable within this pH range, the curve for resonance 4′ strongly suggests proximity of this ring to both basic (pK_a ~ 9) and acidic ($pK_a \lesssim 6$) groups. Trp II has been shown (Llinás et al., 1985; De Marco et al., 1986a) to be a component of the lysine-binding site, which, in turn, is postulated to contain positively and negatively charged titratable side chains providing a electrostatic stabilizing force for binding the dipole ligand (Hochschwender & Laursen, 1981; Trexler et al., 1982). In contrast, the curves for peaks 6′ (His III) and 2′ (Trp I) reveal a relative insensitivity of these two residues to pH. Although this is to be expected for a Trp indole group, a free His imidazolium titrates with pK_a ~ 6. Thus, the His^{33} (His III) side chain appears to be positioned in a structurally shielded locus.

The acid–base responsiveness of the His^{31} and Trp II NH resonances and the relative insensitivities of the corresponding His^{33} and Trp I signals (Figures 4 and 5) are in full agreement with the results obtained from pH titration of the aromatic CH spectrum in ^2H_2O (De Marco et al., 1985c) and the exposures detected by the photo-CIDNP experiments described in the accompanying paper (De Marco et al., 1986b). On the other hand, it is interesting to notice that while all curves in Figure 5 reveal a chemical shift drift at low pH, as expected for an acidic unfolding (De Marco et al., 1985b), the Trp I indole NH peak 2′ does not provide any hint of shifting to its expected random-coil position (~10.1 ppm) down to pH 3, indicating that the Trp I (Trp^{25}?) ring is placed in a structurally stable locus. This conclusion concurs with that from a previous stability study of kringle 4 (De Marco et al., 1985b).

A main aim of this study is to gather evidence as to which residues participate in ligand binding. In discussing the 300-MHz spectra A and B in Figure 1, we have noted that an excess of BASA causes a significant shift of the six low-field NH resonances. The gradual response of the δ <9 ppm spectral region, to increasing additions of BASA, was investigated at 600 MHz. Upon an initial substochiometric addition of ligand, peaks 3′ (unidentified) and 4′ (Trp II) were observed to be the most affected, exhibiting both low-field shifts and broadening at ligand levels corresponding to about half-saturation. The line-width pattern exhibited by peaks 3′ and 4′ is typical of an exchange process by which the kringle structure fluctuates between its ligand-free and BASA-bound states (Feeney et al., 1979). Averaging the chemical shift differences of resonances 3′ and 4′ ($\Delta\delta$ 0.26 and 0.32 ppm, respectively), we can estimate the ligand exchange rate as $(\pi/\sqrt{2})\Delta\delta \sim 400$ Hz, where $\Delta\delta$ refers to the positions of resonances 3′ and 4′ in the free and in the bound kringle states.

The assumption of "moderately fast exchange" between the two states (Jardetzky & Roberts, 1981) enables derivation of the association constant K_a from the monotonic shifts caused by ligand binding. The BASA-concentration dependences of the six NH resonances' chemical shifts under study are plotted

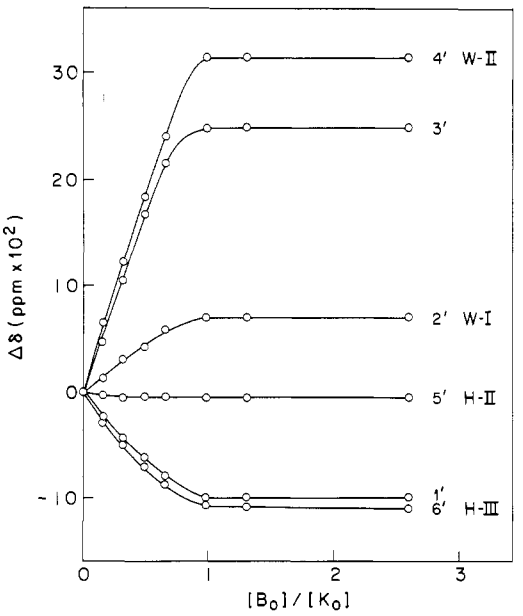

FIGURE 6: BASA titration of kringle 4: ligand-induced chemical shifts on the six low-field exchangeable proton resonances in ^1H_2O. $\Delta\delta$, the chemical shift in the presence of BASA referred to that in the absence of ligand, is plotted vs. $[B_0]/[K_0]$, the ratio of total ligand concentration to total kringle concentration. The experimental data points are extracted from 600-MHz ^{1}H NMR spectra. Kringle concentration $\sim 10^{-3}$ M, pH 7.1, 295 K.

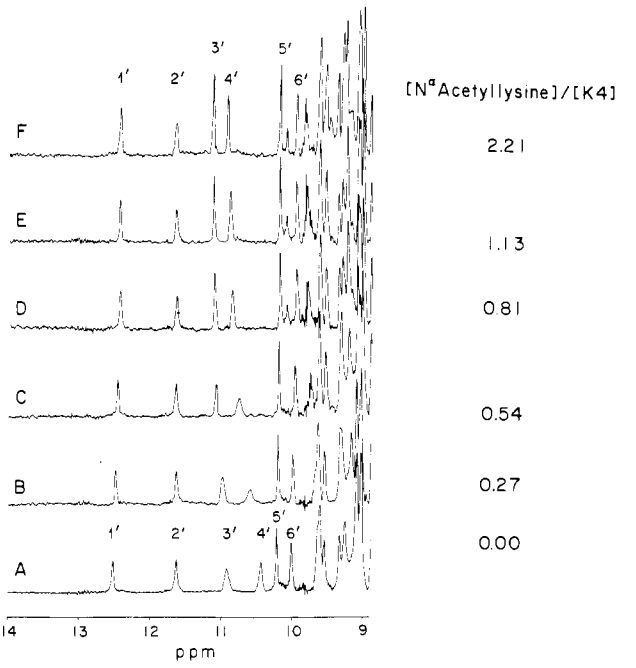

FIGURE 7: ^{1}H NMR low-field spectra of kringle 4 in ^1H_2O, 600 MHz: AcLys titration effects on exchangeable protons. The six resonances under study are numbered 1′–6′. (A) No ligand; (B–F) increasing AcLys concentrations. Kringle concentration $\sim 10^{-3}$ M, pH 7.1, 295 K.

in Figure 6. Assuming one-site binding and a simple Langmuir isotherm saturation profile, the averaged data for the six peaks were used to estimate the BASA–kringle 4 association constant yielding $K_a \sim 79$ mM^{-1}, which is in excellent agreement with $K_a \sim 74$ mM^{-1} reported elsewhere, on the basis of monitoring aromatic CH signals (Hochschwender et al., 1983).

In order to discriminate specific conformational ligand-binding effects, as opposed to anisotropic (ring-current) shifts caused by the effector BASA, the aliphatic ligand analogue N^{α}-acetyl-L-lysine (AcLys) was also investigated (Figure 7). Surprisingly, AcLys causes qualitatively similar effects to those observed for BASA. Thus, a first addition of AcLys (Figure 7B) brings about chemical shift and line-width changes mostly for peaks 3′ and 4′, with marked broadening for peak 4′ (Trp II). As is the case for BASA binding, sharpening is observed on approaching ligand saturation and is extremely pronounced for peaks 3′ and 4′, which now reveal their true singlet character (Figure 7E,F). Figure 8 shows the AcLys titration profile for the chemical shift of the six low-field exchangeable protons. By assuming fast exchange, we estimate $K_a \sim 39$ mM^{-1}, which would indicate a relatively weaker affinity of kringle 4 for the linear ligand when compared to the aromatic one.

CONCLUSIONS

In the accompanying paper (De Marco et al., 1986b) we show how the CIDNP experiment can be exploited to investigate kringle aromatic side chains that are exposed. Specifically, the experiment serves to unveil the rings of His^3, Tyr^{41}, Tyr^{50}, Trp^{72}, and Tyr^{74} as being accessible to the photopolarizable dye. In contrast, the ^{1}H NMR experiments in ^1H_2O described in this paper serve to probe into aromatic groups that are relatively protected, such as Trp^{25}, His^{31}, His^{33}, and Trp^{62}. Because of steric shielding, these groups are not directly accessible via the photo-CIDNP approach. Thus, the information provided by the two techniques complement each other and serve to generate a rough picture for the exposure

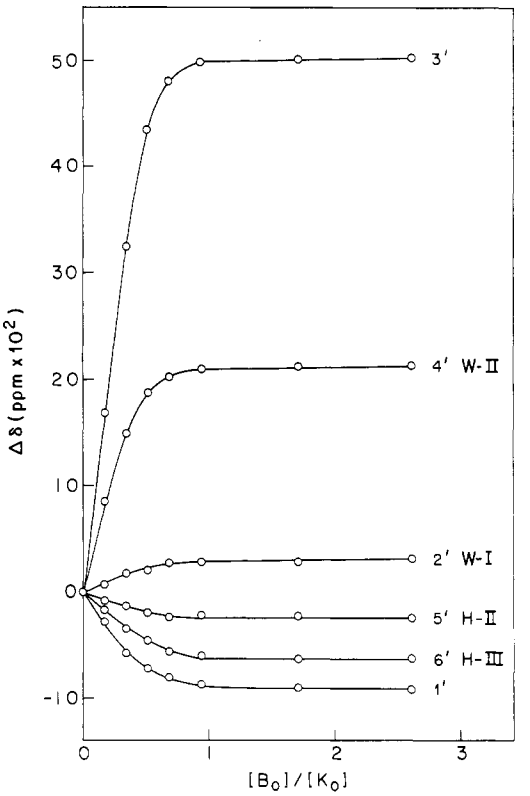

FIGURE 8: ^{1}H NMR AcLys titration of kringle 4: ligand-induced chemical shifts on the six low-field exchangeable proton resonances in ^1H_2O. $\Delta\delta$, the chemical shift in the presence of AcLys referred to that in the absence of ligand, is plotted vs. $[B_0]/[K_0]$, the ratio of total ligand concentration to total protein concentration. The experimental data points are extracted from 600-MHz ^{1}H NMR spectra, examples of which are shown in Figure 7. Kringle concentration $\sim 10^{-3}$ M, pH 7.1, 295 K.

of aromatic residues within the kringle 4 structure.

A summary of the data obtained in this study is listed in Table I. Resonances 5′ (10.20 ppm) and 6′ (10.00 ppm) are

Table I: Chemical Shifts, Assignments, and NOE Connectivities of Low-Field Exchangeable Proton Resonances in Kringle 4[a]

peak[b]	assignment[c]	δ (free)[d]	Δδ (+BASA)[e]	Δδ (+AcLys)[e]	NOE connectivities[f]	
					δ[d]	assignment
1′	unident[g,h]	12.44	−0.10	−0.09	9.99	NH3 His III
					8.31	CH2 His III
					8.88, 8.79, 7.30, 7.20, 7.03	unident[h]
2′	Trp I	11.60	0.07	0.03	7.45	CH7 Trp I
					7.12	CH2 Trp I
					7.27	Phe[64][i]
					8.80, 7.65	unident[h]
3′	unident[h]	10.86	0.25	0.21	7.77	CH2 Trp II
					7.41	Tyr III
					6.84	Tyr II or Tyr IV[i]
					9.21	unident[h]
4′	Trp II	10.43	0.32	0.50	7.77	CH2 Trp II
					7.05	CH7 Trp II
					9.59, 9.21, 9.04, 8.66	unident[h]
5′	His II	10.20	−0.005	−0.02	8.34	CH4 His II
					7.55	CH2 His II
					9.60, 9.02, 8.55, 6.41	unident[h]
6′	His III	10.00	−0.11	−0.06	8.31	CH2 His III
					6.87	CH4 His III
					7.78	CH2 Trp II
					9.06, 7.60	unident[h]

[a] Data extracted from ^1H_2O solutions of kringle 4, pH 7.1, 297 K. [b] NH resonances, labeled as indicated in Figure 1B,D. [c] His and Trp labels indicate imidazole NH3 and indole NH1 resonances, respectively. Trp I and Trp II correspond to Trp[25] and Trp[62] but have not been assigned. His II and His III are assigned to His[31] and His[33], respectively. [d] Chemical shift, in ppm, referred to TSP. [e] Chemical shift, in ppm, for the kringle in the presence of ligand relative to that for the free kringle. [f] NOE connectivities are extracted from the Overhauser experiments shown in Figure 2. [g] Doublet, $J \sim 7.9$ Hz. [h] Unidentified exchange-labile NH. [i] Tentative assignment; signal may also arise from an unidentified NH group.

shown to arise from His side-chain NH3 sites. This is in agreement with previous studies (Reynolds et al., 1973; Blomberg et al., 1977; Stoesz et al., 1979; Munowitz et al., 1982) showing that the imidazole N3 site (tautomer A, Scheme I) is predominant under basic conditions (pH > pK_a). Resonance 1′ (12.44 ppm) is most conspicuous as it is severely shifted to low field and exhibits a neat doublet character ($J \sim 7.9$ Hz). Because it yields a good NOE on the His III (His[33]) CH2 signal (Figure 2A), it may be suggested that it arises from the His III imidazole NH1 site. This interpretation is particularly appealing since the His III imidazole does not titrate within the range 2.5 < pH < 11.0, which suggests that it has a rather extreme pK_a (De Marco et al., 1985c). However, its splitting indicates that the potentially coupled CH2 signal should also be a doublet, for which we observe no clear evidence in the ^1H_2O spectrum nor in decoupling experiments where the NH transition was irradiated. Thus, we are tentatively identifying this resonance as an amide NH, which is structurally close to the His III ring. In the ferrichrome peptides we have observed an intramolecularly H-bonded amide NH signal shifted to ~10 ppm in water and ~11 ppm in trifluoroethanol, which further deshields the proton by solvent H bonding to the peptidyl C=O group (Llinás & Klein, 1975). Thus, it is not inconceivable that further deshielding might occur if the NH group were positioned close to an aromatic ring.

Inspection of Figures 6 and 8 indicates that resonances 3′ and 4′ (Trp II) are low-field-shifted to different extents by the two ligands. Proton Overhauser experiments have shown that the Trp II indole is in direct contact with the BASA ring (Llinás et al., 1985), which would be consistent with the larger shift of peak 4′ being contributed by an anisotropic ring current effect of the aromatic ligand. The relatively more pronounced shift of peak 3′ in presence of AcLys (Figure 8) could also result from a similar effect, whereby the BASA ring would magnetically shield (rather than deshield, as is the case for peak 4′) the peak 3′ NH site. Peaks 1′, 2′ (Trp I), 5′ (His[31]), and 6′ (His[33]) are not much affected by either ligand, suggesting that they originate from protons not in contact with the effectors and/or that they sense ligand presence only indirectly, through conformational rearrangements of neighbor side chains. At any rate, the ~0.5 ppm resonance shift induced by AcLys on the as yet unidentified peak 3′ (Figure 8) suggests that this exchange-labile NH group may play some direct role in ligand binding. This will be the subject of a separate study.

Registry No. BASA, 2393-24-0; L-AcLys, 1946-82-3; L-His, 71-00-1; L-Trp, 73-22-3; plasminogen, 9001-91-6.

References

Alexander, S. (1968) *Rev. Sci. Instrum. 39*, 1066.

Blomberg, F., Maurer, W., & Rüterjans, H. (1977) *J. Am. Chem. Soc. 99*, 8149–8159.

Clore, G. M., Kimber, B. J., & Gronenborn, A. M. (1983) *J. Magn. Reson. 54*, 170–173.

De Marco, A. (1977) *J. Magn. Reson. 26*, 527–528.

De Marco, A., Laursen, R. A., & Llinás, M. (1985a) *Biochim. Biophys. Acta 827*, 369–380.

De Marco, A., Motta, A., Laursen, R. A., & Llinás, M. (1985b) *Biophys. J. 48*, 411–422.

De Marco, A., Pluck, N. D., Bányai, L., Trexler, M., Laursen, R. A., Patthy, L., Llinás, M., & Williams, R. J. P. (1985c) *Biochemistry 24*, 748–753.

De Marco, A., Laursen, R. A., & Llinás, M. (1986a) *Arch. Biochem. Biophys. 244*, 727–741.

De Marco, A., Zetta, L., Petros, A. M., Llinás, M., Boelens, R., & Kaptein, R. (1986b) *Biochemistry* (preceding paper in this issue).

Dubs, A., Wagner, G., & Wüthrich, K. (1979) *Biochim. Biophys. Acta 577*, 177–194.

Ernst, R. R. (1966) *Adv. Magn. Reson. 2*, 1–135.

Feeney, J., Batchelor, J. G., Albrand, J. P., & Roberts, G. C. K. (1979) *J. Magn. Reson. 33*, 519–529.

Ferrige, A. G., & Lindon, J. C. (1978) *J. Magn. Reson. 31*, 337–340.

Hochschwender, S. M., & Laursen, R. A. (1981) *J. Biol. Chem. 256*, 11172–11176.

Hochschwender, S. M., Laursen, R. A., De Marco, A., & Llinás, M. (1983) *Arch. Biochem. Biophys. 223*, 58–67.
Jardetzky, O., & Roberts, G. C. K. (1981) *NMR in Molecular Biology*, Chapter 4, Academic, New York.
Lerch, P. G., & Rickli, E. E. (1980) *Biochim. Biophys. Acta 625*, 374–378.
Lerch, P. G., Rickli, E. E., Lergier, W., & Gillesen, D. (1980) *Eur. J. Biochem. 107*, 7–13.
Llinás, M., & Klein, M. P. (1975) *J. Am. Chem. Soc. 97*, 4731–4737.
Llinás, M., De Marco, A., Hochschwender, S., & Laursen, R. A. (1983) *Eur. J. Biochem. 135*, 379–391.
Llinás, M., Motta, A., De Marco, A., & Laursen, R. A. (1985) *J. Biosci. 8*, 121–139.
Markley, J. L. (1975) *Acc. Chem. Res. 8*, 70–80.
Munowitz, M., Bachovnin, W. W., Herzfeld, J., Dobson, C. M., & Griffin, R. G. (1982) *J. Am. Chem. Soc. 104*, 1192–1196.
Poulsen, F. M., Hoch, J. C., & Dobson, C. M. (1980) *Biochemistry 19*, 2597–2607.
Ramesh, V., Gyenes, M., Patthy, L., & Llinás, M. (1986) *Eur. J. Biochem. 159*, 581–595.
Redfield, A. G., & Gupta, R. K. (1971) *J. Chem. Phys. 54*, 1418–1419.
Reynolds, W. F., Peat, I. R., Freedman, M. H., & Lyerla, J. R. (1973) *J. Am. Chem. Soc. 95*, 328–331.
Roth, K., Kimber, B. J., & Feeney, J. (1980) *J. Magn. Reson. 41*, 302–309.
Sottrup-Jensen, L., Claeys, H., Zajdel, M., Petersen, T. E., & Magnusson, S. (1978) *Prog. Chem. Fibrinolysis Thrombolysis 3*, 191–209.
Stoesz, J. D., Malinowski, D. P., & Redfield, R. (1979) *Biochemistry 18*, 4669–4675.
Thorsen, S., Clemmensen, I., Sottrup-Jensen, L., & Magnusson, S. (1981) *Biochim. Biophys. Acta 668*, 377–387.
Trexler, M., Váli, Z., & Patthy, L. (1982) *J. Biol. Chem. 257*, 7401–7406.
Trexler, M., Bányai, L., Patthy, L., Pluck, N. D., & Williams, R. J. P. (1983) *FEBS Lett. 154*, 311–318.
Trexler, M., Bányai, L., Patthy, L., Pluck, N. D., & Williams, R. J. P. (1985) *Eur. J. Biochem. 152*, 439–446.
Wiman, B., & Wallén, P. (1977) *Thromb. Res. 10*, 213–222.
Winn, E. S., Hu, S.-P., Hochschwender, S. M., & Laursen, R. A. (1980) *Eur. J. Biochem. 104*, 579–586.

Thermodynamics of Dimer and Tetramer Formations in Rabbit Muscle Phosphofructokinase†

Michael A. Luther,‡ Guang-Zuan Cai, and James C. Lee*
E. A. Doisy Department of Biochemistry, St. Louis University School of Medicine, St. Louis, Missouri 63104
Received April 2, 1986; Revised Manuscript Received August 1, 1986

ABSTRACT: The self-association of rabbit muscle phosphofructokinase (PFK) was monitored as a function of temperature, pH, and ionic strength in order to understand the thermodynamics of this aggregation process. Thermodynamic parameters obtained from the temperature study show that the dimerization of PFK is characterized by negative entropy and enthalpy changes of -270 ± 5 eu and -87 ± 1 kcal/mol, respectively, with no observable change in heat capacity. This is in contrast to the formation of the tetramer, which is governed by positive entropy and enthalpy changes and a positive heat capacity change of 5000 ± 2000 cal/mol. Low ionic strength also favors the formation of the dimer without a significant influence on the tetramerization, which is enhanced by increasing the pH from 6.00 to 8.55. Furthermore, Wyman linkage analysis [Wyman, J. (1964) *Adv. Protein Chem. 19*, 224–285] reveals that the formation of the tetramer from the monomer between pH 6.00 and pH 8.55 involves the loss of 3.3 protons. Further analysis shows that ionization of residues with an apparent pK_a of 6.9 is linked to the formation of PFK tetramers. The conclusion of this study indicates that the major noncovalent forces governing the formation of the dimer are different from those for the association of the tetramer.

The self-association of rabbit muscle phosphofructokinase (PFK)[1] has been the topic of many investigations by a variety of techniques (Parmeggiani et al., 1966; Ling et al., 1965; Leonard & Walker, 1972; Pavelich & Hammes, 1972; Goldhammer & Paradies, 1979; Hesterberg & Lee, 1981, 1982; Luther et al., 1983, 1985). One of the goals for such intensive investigation is to elucidate the role of self-association in the regulation of enzyme activity. Recently, there is an increasing number of reports to indicate that the kinetic properties of PFK are dependent on protein concentrations (Reinhart, 1984; Luther et al., 1985). Hence, an elucidation of the mechanism of regulation of PFK activity is linked to a knowledge on the basic thermodynamics that govern the self-association of PFK.

Luther et al. (1985) showed that, within the limits of resolution by sedimentation velocity, *active* PFK undergoes reversible self-association and the various oligomeric species are in a rapid, dynamic equilibrium. In conjunction with other reports from the literature and this laboratory, it was shown

† Supported by National Institutes of Health Grants AM-21489 and NS-14269.
‡ Present address: The Salk Institute, San Diego, CA 92138.

[1] Abbreviations: PFK, phosphofructokinase; 3× TEMA buffer, 75 mM Tris–carbonate, 18 mM $MgCl_2$, 9 mM $(NH_4)_2SO_4$, and 3 mM EDTA; IEMA buffer, 75 mM imidazole, 18 mM $MgCl_2$, 9 mM $(NH_4)_2SO_4$, and 3 mM EDTA at pH 7.0; Tris, tris(hydroxymethyl)-aminomethane; EDTA, ethylenediaminetetraacetic acid.

0006-2960/86/0425-7931$01.50/0